# Distributed Power Allocation for Interference Limited Networks

Cédric Abgrall[†‡], Emilio Calvanese Strinati[†] and Jean-Claude Belfiore[‡]
Email: cedric.abgrall@cea.fr, emilio.calvanese-strinati@cea.fr and jean-claude.belfiore@telecom-paristech.fr

[†]CEA, LETI, MINATEC
17, rue des Martyrs - 38054 Grenoble, France

[‡]TELECOM ParisTech
46, rue Barrault - 75013 Paris, France

## ABSTRACT

***Abstract*—The goal of our work is to limit in-band interference in wireless communication systems. Based on a three-regime interference classifier, we propose a novel distributed inter-cell power allocation algorithm where each cell computes by an iterative process its minimum power budget to meet its local quality of service (QoS) constraints. Analytical results show how our proposal permits to notably reduce both transmission power and harmful effects of in-band interference, while meeting QoS constraints of users in each cell.**

***Index Terms*—Interference limited networks, power allocation, resource management, interference mitigation.**

## I. INTRODUCTION

Future wireless communication systems target high capacity transmissions in interference limited scenarios. Furthermore, network operators have to guarantee QoS to customers in increasingly dense cellular systems. The interference issue becomes a detrimental and QoS-limiting bottleneck.

Several methods have been proposed to limit prejudicial effects of interference experienced by destinations; main techniques are surveyed and commented below. First, Resource Allocation Management can avoid in-band concurrent transmissions to cause intra-cell and inter-cell interference by full time/frequency orthogonalization of transmission resources. Nevertheless, such orthogonal allocation techniques may result in poor resource reuse. More flexible approaches are promising: Frequency Reuse [1], for instance, consists in reallocating part of frequency resources in adjacent spatial locations. Second, signal processing techniques such as Dirty Paper Coding, Successive Interference Cancellation, Sphere Decoder or Interference Alignment (IA) can help in coping with detrimental effects of interference [2]–[5]. Recently, with its challenging results, IA relaunches interest for interference mitigation processing. Nevertheless, such techniques present complex implementation and a full knowledge of Channel State Information (CSI) is required. Third, interference can be fought by channel aware adaptive mechanisms such as Adaptive Modulation Coding (AMC) [6] and Power Control. For instance, Water-Filling [7] is proposed to optimize a cost function under a set of constraints. Such a technique is based on Game Theory and Convex Optimization [8][10]. Indeed, any power variation in a cell affects perceived inter-cell interference in neighbour cells, which will react by adjusting their own power, and so on.

Most previous work in the domain of power allocation for interference mitigation focuses on centralized techniques [10]–[12]. Centralized approaches can perform optimally. Nevertheless, the presence of a centralized network controller (NC), that dictates the power allocated to each cell, is needed. With centralized techniques, base stations (BS) first inform NC on channel quality with user equipments (UE). Then, NC estimates the optimum power allocation level for each BS. Finally, NC broadcasts to BSs the decision on the momentary power allocation set. Centralized approaches have three main drawbacks. First, effectiveness of such approaches depends on the reliability of estimation of link quality between each node (BS and UE). Second, signalling (for channel estimation) and control overhead (broadcast of power allocation set) is introduced. Third, all computation complexity is carried out at NC. Power allocation can also be computed with a distributed algorithm. Distributed techniques have been mainly investigated in the literature for reducing both channel estimation and inter-cell signalling. But sometimes a centralized NC may simply be infeasible (or not desired). Distributed power allocation techniques may suffer from sub-optimality and computation time. Their main drawback is the amount of CSI required at each BS. Commonly, BSs periodically refresh their CSI estimation on locally active UEs to perform link adaptation techniques (AMC, power control, channel aware scheduling, etc.). If BSs need additional information on neighbour interfering cells, extra dedicated monitoring and consequent signalling is required.

In the literature, some theoretical investigations propose to classify perceived interference at UE in five regimes, namely *noisy*, *weak*, *moderately weak*, *strong* and *very strong* interference regimes [13][14]. Furthermore, Han and Kobayashi proposed in [15] to decompose, at the coder, messages into a *private* part for an exclusive UE and a *common* part decodable by all UEs. The proportion of private and common information in the global message can be matched up with the interference classification. For instance, messages are entirely *private* in the *noisy* regime, while they are entirely *common* in the *very strong* regime. The combination of *private* and *common* messages at the coder is achieved by superposition coding. Nevertheless, such a five-regime classifier, as well as superposition coding, require complex processing which cannot be met in practice. Therefore, in-band inter-cell interference is mostly processed in practice by a single (and not necessarily optimal) interference mitigation scheme. Particularly, most

978-1-4244-8016-6/10/$26.00 ©2010 IEEE

power control algorithms in interfered networks consider in-band interference as additional noise (*noisy* regime).

The contribution of this paper is twofold. First, we present a novel simplified and effective interference classifier (Section III). Second, we exploit such an interference classifier to define a distributed power allocation (DPA) algorithm (Section IV) which minimizes the power budget in an interference limited multi-cell network under QoS constraints.

## II. Notations and System Model

In our work, we consider a system with two neighbour cells, $\mathscr{C}_1$ and $\mathscr{C}_2$, whose downlink transmissions occur over a common communication band. Each cell $\mathscr{C}_i$ consists of a base station (source $s_i$) and a single user equipment (destination $d_i$), both are single-antenna. Besides, $\mathscr{C}_i$ is rate and power constrained, *i.e.*, $s_i$ must ensure at least the target information rate $\mathbf{R_i}$ for $d_i$, while transmission power $P_i$ at $s_i$ cannot exceed the system limitation $\mathbf{P_{i,max}}$ (*constraints are bold faced*). Our interference limited system is modelled as the Interference Channel (IC) [15] illustrated on Figure 1a: communication rates are limited by inter-cell interference and Gaussian noise $z_i \sim \mathcal{N}(0, N_0)$. Destination $d_i$ is assumed able to decode the interfering message $x_j$ sent by $s_j$, even if the information message $x_i$ from $s_i$ is the one dedicated to $d_i$. As a consequence, the information rate $\mathbf{R_j}$ of the interfering cell $\mathscr{C}_j$ is assumed to be known by $\mathscr{C}_i$. The received signal at $d_i$ is given by

$$y_i = g_{i,i} \cdot x_i + g_{j,i} \cdot x_j + z_i$$

where the channel gain $g_{k,l}$ between $s_k$ and $d_l$ is assumed quasi-static and slow-varying (slow fading, low mobility). Concerning CSI assumptions, destinations just need to estimate their Signal to Noise Ratio (SNR) and Interference to Noise Ratio (INR), while sources need link quality of their user. No signalling between cells is assumed.

Focusing on destination viewpoint, our system can be divided into two many-to-one IC denoted by $(\Delta_i)_{i=1,2}$. Subsystem $\Delta_i$ accounts for the whole cell $\mathscr{C}_i$ with its interfering neighbour source $s_j$. $\Delta_1$ is illustrated on Figure 1b and seems to be the well-known two-user Multiple Access Channel (MAC) [16]. Nevertheless, $\Delta_i$ differs from a two-user MAC. Indeed, with a MAC, both sources send intentionally information to the common destination, whereas with $\Delta_i$, the crossed channel $(g_{j,i})$ conveys interference instead of information. Furthermore, a MAC tries to optimize rates pair $(R_1; R_2)$, whereas $\Delta_i$ cannot control crossed rate $R_j$ and has to deal with $R_j$ without reducing $R_i$. So as to insist on these fundamental differences between a MAC and $\Delta_i$, we refer, for system $\Delta_i$, to information and crossed rates respectively as $\rho_i$ and $\mu_i$, instead of $R_i$ and $R_j$. But we have $\mu_i = \rho_j = R_j$ in practice.

Finally, variables $A_i$, $B_i$, $C_i$ and $A$ used hereafter are introduced, while $\gamma_i$ and $\delta_i$ respectively denote SNR and INR perceived at $d_i$.

$$\gamma_i = \frac{g_{i,i} \cdot P_i}{N_0}, \quad \delta_i = \frac{g_{j,i} \cdot P_j}{N_0} = f_j \cdot \gamma_j \text{ with } f_j = \frac{g_{j,i}}{g_{j,j}} \tag{1}$$

$$A_i = 2^{\rho_i} - 1, \quad B_i = 2^{\mu_i} - 1 = A_j \tag{2}$$

$$C_i = 2^{\rho_i + \mu_i} - 1 = (A_i + 1)(B_i + 1) - 1 = A \tag{3}$$

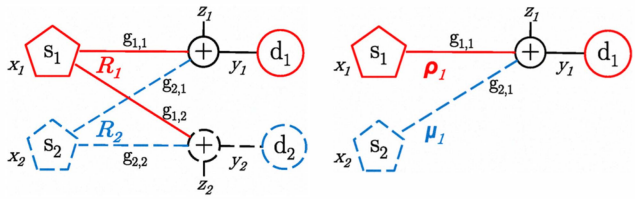


(a) Two-user Interference Channel (b) $\Delta_1$: Many-to-one IC

Fig. 1: Adopted system models for $\mathscr{C}_1$ and $\mathscr{C}_2$

## III. Proposed Simplified Interference Classification

In this section, we propose a simplified interference classification which reduces the processing complexity in comparison to the classification in [13]–[15]. Since *private* and *common* data flows cannot be superposed in practice, we force the sources to output a single *common* flow. To this end, we assumed the destinations can decode interfering messages. However, the decoding process at destination $d_i$ is adapted to its perceived INR $\delta_i$: the decoder treats interfering message $x_j$ either as a *private* or as a *common* message. We classify interference into three regimes. Either, the interference signal is 'weak' (roughly at noise level) (see III-A). In this case we process interference as additional noise. Otherwise, we decode interference, either before processing the intended signal (see III-B.1), or jointly with the intended signal (see III-B.2). Each destination can, in an autonomic way, classify its momentary perceived interference and consequently choose how to process interfering signal without relying on specific information from a central decision maker.

MAC and IC performance is typically characterized by their capacity region, which is the set of all simultaneously achievable rates pairs $(R_1; R_2)$, *i.e.*, rates that can be transmitted with arbitrarily small error probability. Capacity region upper bounds have been proposed for MAC and IC in [13]–[17]; some of these bounds are used below to introduce our three-regime interference classifier for subsystem $\Delta_i$. For each regime, we derive first the region where the regime is applicable, second performance that can be achieved.

### A. "Noisy" Interference Regime

The *noisy* regime corresponds to the most conventional way for processing interference, *i.e.*, as thermal noise. Applicability of this regime is related to the incapacity of $d_i$ to decode the neighbour message $x_j$ (see (4): channel in outage). If the perceived neighbour signal is too weak, then processing $x_j$ as additional noise is optimal (see (5): INR at denominator).

Equation (4) specifies the region where this regime is consistent, while equation (5) exhibits an upper bound for the achievable information rate $\rho_i$. Performance can be expressed either in terms of rates with $\rho_i$ and $\mu_i$, or in terms of SNR with $\gamma_i$ and $\gamma_j = \frac{1}{f_j} \cdot \delta_i$.

$$\mu_i \geq \log_2(1 + \delta_i) \quad \Leftrightarrow \quad f_j \cdot \gamma_j \leq B_i \tag{4}$$

$$\rho_i \leq \log_2\left(1 + \frac{\gamma_i}{1 + f_j \cdot \gamma_j}\right) \quad \Leftrightarrow \quad \gamma_i \geq A_i(1 + f_j \cdot \gamma_j) \tag{5}$$

### B. "MAC-like" Interference Regimes

If perceived interference is not classified as *noisy*, then we decode both messages, as a two-user MAC would make it ("MAC-like"). The capacity region of the two-user MAC can thus be exploited to evaluate our performance. This region is bounded by the individual rates of each intended source and by the sum of these rates (sum-rate), as shown in (6)-left. The capacity region of $\Delta_i$ can be then derived as (6)-right. The second inequality in (6)-R does not hold since the crossed link conveys interference instead of information; there is thus no reason for $\Delta_i$ to limit its performance to the achievable rate over this interfering link. So, only two inequalities are relevant in practice. Hereafter we derive their performance.

$$\left\{\begin{array}{l} R_1 \leq \log_2(1+\gamma_1) \\ R_2 \leq \log_2(1+\gamma_2) \\ R_1+R_2 \leq \log_2(1+\gamma_1+\gamma_2) \end{array}\right. \Leftrightarrow \left\{\begin{array}{l} \rho_i \leq \log_2(1+\gamma_i) \\ \mu_i \leq \log_2(1+\delta_i) \\ \rho_i+\mu_i \leq \log_2(1+\gamma_i+\delta_i) \end{array}\right. \quad (6)$$

*B.1) "Interference Cancellation" Regime:* Here, interference is so strong that it causes no degradation in comparison to a scenario without interference. Such a regime is known in the literature as the *very strong* interference regime [18]. Optimal scheme consists in first decoding interfering data while treating information data as noise, then subtracting interference to the received signal and eventually decoding the information signal cleaned from interference. Interference is then cancelled out. Equation (7) specifies the applicability range of this regime while (8) bounds the achievable information rate $\rho_i$ and SNR $\gamma_i$. Referring to (6)-R this regime stands for the first inequality.

$$\mu_i \leq \log_2\left(1+\frac{\delta_i}{1+\gamma_i}\right) \quad \Leftrightarrow \quad f_j \cdot \gamma_j \geq B_i(1+\gamma_i) \quad (7)$$

$$\rho_i \leq \log_2(1+\gamma_i) \quad \Leftrightarrow \quad \gamma_i \geq A_i \quad (8)$$

*B.2) "Jointly Decoding" Regime:* With this regime, perceived inter-cell interference is not strong enough to be decoded alone and not weak enough to be treated as noise; destination jointly decodes information and interference for recovering the information signal. This regime is jammed between *noisy* and *interference cancellation* regimes:

$$\begin{array}{l} \log_2\left(1+\frac{\delta_i}{1+\gamma_i}\right) \leq \mu_i \leq \log_2(1+\delta_j) \\ \Leftrightarrow \quad \frac{f_j \cdot \gamma_j}{1+\gamma_i} \leq B_i \leq f_j \cdot \gamma_j \end{array} \quad (9)$$

Achievable $\rho_i$ and $\gamma_i$ are derived from the third line of (6)-R:

$$\rho_i \leq \log_2(1+\gamma_i+f_j\cdot\gamma_j)-\mu_j \quad \Leftrightarrow \quad \gamma_i \geq C_i - f_j\cdot\gamma_j \quad (10)$$

### C. Achievable SNR Region for $\mathscr{C}_i$

Performance of our three-level interference classification is illustrated hereafter. Since in practice $\mu_i = \rho_j = \mathbf{R_j}$ holds, variables $B_i$ and $C_i$ are useless (see (2)-(3)). Furthermore, each regime is completely defined by knowledge of couples $(\gamma_i;\delta_i)$ and $(\mathbf{R_1};\mathbf{R_2})$ (see (4)–(10)). Therefore, the parameters set $\mathscr{P}_S = \{\mathbf{R_1};\mathbf{R_2};\mathbf{f_1};\mathbf{f_2}\}$ states performance for $\mathscr{C}_1$ and $\mathscr{C}_2$.

Usually, the optimization problem of rate maximization under power constraints is characterized by its achievable capacity region in region $(R_1;R_2)$. Since we seek to optimize the dual problem, *i.e.*, minimizing transmission power while meeting rates $(\mathbf{R_1},\mathbf{R_2})$, it suits better to derive the achievable power region. $P_i$ is easily deduced from $\gamma_i$ with (1). So we rather work in region $(\gamma_i;\delta_i)$ (recall: $\delta_i = f_j\cdot\gamma_j$) within which we derive the achievable SNR region $\mathscr{R}_i^*$, *i.e.*, the set of all pairs $(\gamma_i;\delta_i)$ that let $\Delta_i$ (or equivalently, $\mathscr{C}_i$) meet its target rate $\mathbf{R_i}$. Our optimization problem is described by (5), (8), (10) respectively subject to constraints (4), (7), (9) defining three adjacent and non-overlapping regions (coloured respectively in yellow, green and white on Figure 2).

$\mathscr{R}_i^*$ is shown on Figure 2, where $\gamma_{i,max}$ and $\delta_{i,max}$ state limitations $\mathbf{P_{i,max}}$ and $\mathbf{P_{j,max}}$. Dash-dot red lines illustrate the applicability boundaries (4) and (7) of the three regimes. Solid blue lines $(\mathscr{D}_i^k)_{k=1..3}$ show the lower bounds (5), (10) and (8) of $\mathscr{R}_i^*$, respectively for the *noisy*, *joint decoding* and *interference cancellation* regimes. The blended shades of blue specify that $\mathscr{R}_i^*$ is located above blue lines $(\mathscr{D}_i^k)_k$. Nevertheless minimizing power $P_i$ implies minimizing $\gamma_i$; optimal solution to our problem is so located on lines $(\mathscr{D}_i^k)_k$, *i.e.*, (5), (8) and (10) are taken as equalities instead of inequalities. Figure 2 is obtained for a given communication scenario $\mathscr{P}_S$; changing one parameter in $\mathscr{P}_S$ impacts lines equations.

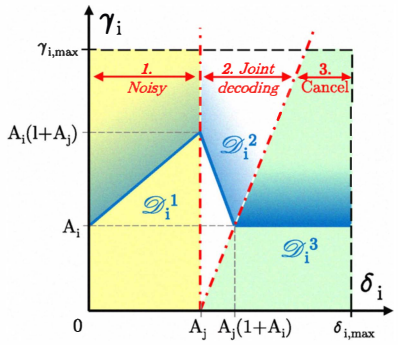


Fig. 2: Achievable SNR region $\mathscr{R}_i^*$ for $\mathscr{C}_i$

## IV. Proposed Distributed Power Allocation (DPA) Algorithm

According to information theory, perceived interference at destination can be classified into different operating regimes. In each regime, interference can be conveniently processed. However, most previous work on power allocation adopts a single interference regime [10]–[12]. Such approaches fail as soon as perceived interference is not consistent any more with the applicability region of the regime; some transmissions must then be rejected. Based on these observations, we propose to classify on an autonomic way the momentary perceived interference in each cell. Thus, each source can in turn efficiently update and minimize its transmission power under its QoS constraint, without any extra signalling. Power is allocated by an iterative "ping-pong" process (see Fig.3b) whose convergence is proved in Section V. Main steps of our DPA algorithm are summarized as follows:

**Step 1.** $s_1$ and $s_2$ broadcast their target rate $\mathbf{R_1}$ and $\mathbf{R_2}$.
**Step 2.** The power allocation set is initialized at $n=0$ with $\underline{P}^0 = (\mathbf{P_{1,max}};\mathbf{P_{2,max}})$. $\mathscr{C}_i$ starts the process.
**Step 3.** $d_i$ estimates $\gamma_i^n$ and classifies its perceived $\delta_i^n$.
**Step 4.** $d_i$ notifies $s_i$ of $\delta_i^n$ and its relevant regime $O_i^n$.

**Step 5.** $s_i$ updates $P_i^n$ on $P_i^{n+1}$, based on $\delta_i^n$ and $O_i^n$.
**Step 6.** $d_j$ estimates $\gamma_j^n$ and classifies its perceived $\delta_j^{n+1}$.
**Step 7.** $d_j$ notifies $s_j$ of $\delta_j^{n+1}$ and its relevant regime $O_j^n$.
**Step 8.** $s_j$ updates $P_j^n$ on $P_j^{n+1}$, based on $\delta_j^{n+1}$ and $O_j^n$.
**Step 9.** $\underline{\Gamma}^{n+1} \leftarrow (\gamma_1^{n+1}; \gamma_2^{n+1}), \underline{P}^{n+1} \leftarrow (P_1^{n+1}; P_2^{n+1}), n \leftarrow n+1$.
*Steps 3–9 are repeated until* $\|\underline{\Gamma}^{n+1} - \underline{\Gamma}^n\| < \varepsilon$ *or* $n \leq n_{MAX}$.

## V. Convergence of DPA: Analytical and Numerical Evaluations

In this section we show that the proposed DPA algorithm most of the time converge to an optimal solution. Furthermore, we investigate some main convergence features of DPA. To this end, we first recall the main mathematical tools needed to understand our proposal. Second, we explain how to apply such theoretical mathematical tools to the system model presented in Section II. Third, we outline the applicability constraints of the proposed method to our system model.

### A. Recall of the Banach Fixed Point Theorem

Let $u : X \to X$ be a mapping from a set $X$ to itself. An *iterated function sequence* $(u^n)_n$ is defined as

$$\begin{cases} u^0 = id_X \\ u^n = u \circ u^{n-1} \end{cases}$$

where $id_X$ is the identity function on $X$ and $(u \circ v)$ is a composed function, *i.e.*, $(u \circ v)(x) = u\left[(v(x)\right]$. Any sequence is derived from $(u^n)_n$ by its first value $x_0$ and recurrence

$$x_n = u\left(x_{n-1}\right) = u^n\left(x_0\right).$$

Let $u : E \to E$ be a mapping from a metric space $(E, d)$ to itself; $d$ is the metric on $E$. $u$ is called a *contraction* if there is some real number $\kappa < 1$ such that (11) is satisfied.

$$\forall (x; y) \in E \times E, \quad d\Big(u(x), u(y)\Big) \leq \kappa \cdot d(x, y) \qquad (11)$$

The smallest value of $\kappa$ is called the *Lipschitz constant* of $u$; a fixed point for $u$ is a point $x^*$ in $E$ invariant under $u$, *i.e.*, $u(x^*) = x^*$. The *Banach fixed point* theorem proves existence and uniqueness of a limit for such recurrent sequences [19].

**Theorem.** *If $(E, d)$ is a non-empty complete metric space and $u : E \to E$ is a contraction with a Lipschitz constant $\kappa < 1$, then $u$ admits one and only one fixed point $x^*$ in $E$. Furthermore, the iterated function sequence $(x_0, u(x_0), u^2(x_0), \cdots)$ converges to $x^*$, whatever $x_0$ may be. The fixed point $x^*$ is also called an attractor.*

### B. Applicability of Banach Theorem to our System Model

Solutions to our optimization problem for $\mathscr{C}_i$, subject to our interference classifier, are derived as (12). For each regime $k \in \{1; 2; 3\}$, transmission power $P_i^n$ at iteration $n$ is minimized under constraint $\mathbf{R_i}$ by a mapping $u_i^k$, within its region of applicability, such that $\gamma_i^{n+1} = u_i^k(\delta_i^n)$. Since applicability regions are disjointed (see Fig. 2), only one regime is relevant in $\mathscr{C}_i$ at iteration $n$ for the momentary $\underline{\Gamma}^n = (\gamma_1^n; \gamma_2^n)$ and fixed scenario $\mathscr{P}_S$; this classified regime is named by $O_i^n$. Thus, $\gamma_i^n$ is updated with the mapping $u_i^{O_i^n}$, based on the momentary perceived inter-cell interference $\delta_i^n = f_j \cdot \gamma_j^n$. Power $P_i^n$ is minimal since any power lower than $P_i^n$ cannot meet $\mathbf{R_i}$.

| $O_i$ | $O_j$ | $\Phi_i(\gamma_i) = (u_i^{O_i} \circ u_j^{O_j})(\gamma_i)$ | $\gamma_i^*$ |
|---|---|---|---|
| 1 | 1 | $A_i A_j f_i f_j \cdot \gamma_i + A_i(1 + A_j f_j)$ | $\frac{A_i(1+A_j f_j)}{1-A_i A_j f_i f_j}$ |
| 1 | 2 | $-A_i f_i f_j \cdot \gamma_i + A_i(1 + A f_j)$ | $\frac{A_i(1+A f_j)}{1+A_i f_i f_j}$ |
| 1 | 3 | $A_i(1 + A_j f_j)$ | $A_i(1 + A_j f_j)$ |
| 2 | 1 | $-A_j f_i f_j \cdot \gamma_i + A - A_j f_j$ | $\frac{A - A_j f_j}{1+A_j f_i f_j}$ |
| 2 | 2 | $f_i f_j \cdot \gamma_i + A(1 - f_j)$ | $\frac{A(1-f_j)}{1-f_i f_j}$ |
| 2 | 3 | $A - A_j f_j$ | $A - A_j f_j$ |
| 3 | 1 | $A_i$ | $A_i$ |
| 3 | 2 | $A_i$ | $A_i$ |
| 3 | 3 | $A_i$ | $A_i$ |

TABLE I: Updating mapping $\Phi_i$ and its attractor $\gamma_i^*$

$$\begin{aligned} &\text{1. Noisy} && \begin{cases} u_i^1 : \gamma_i = A_i\left(1 + f_j \cdot \gamma_j\right) \\ \gamma_j \leq \frac{A_j}{f_j} \end{cases} \\ &\text{2. Jointly decoding} && \begin{cases} u_i^2 : \gamma_i = A - f_j \cdot \gamma_j \\ \frac{A_j}{f_j} \leq \gamma_j \leq \frac{A_j}{f_j}\left(1 + \gamma_i\right) \end{cases} \\ &\text{3. Interference Cancellation} && \begin{cases} u_i^3 : \gamma_i = A_i \\ \gamma_j \geq \frac{A_j}{f_j}\left(1 + \gamma_i\right) \end{cases} \end{aligned} \qquad (12)$$

DPA needs a "ping-pong" process. Update of $(\gamma_i^n)_n$ is indeed derived as an iterated function sequence ($\mathscr{C}_1$ starts):

$$\begin{cases} \gamma_1^n = u_1^{O_1^n}(\gamma_2^{n-1}) \\ \gamma_2^n = u_2^{O_2^n}(\gamma_1^n) \\ \gamma_1^{n+1} = u_1^{O_1^{n+1}}(\gamma_2^n) \\ \gamma_2^{n+1} = u_2^{O_2^{n+1}}(\gamma_1^{n+1}) \end{cases} \Rightarrow \begin{cases} \gamma_1^{n+1} = \Phi_1(\gamma_1^n) \\ \gamma_2^{n+1} = \Phi_2(\gamma_2^n) \end{cases} \qquad (13)$$

with the composed mapping $\Phi_i = (u_i^{O_i^{n+1}} \circ u_j^{O_j^n})$. The expression of $\Phi_i$ therefore depends on the momentary interference scenario $(O_i^{n+1}; O_j^n)$. Table I details all possible derivations of $\Phi_i$ and its attractor $\gamma_i^*$ which is the solution to $\Phi_i(\gamma_i^*) = \gamma_i^*$.

### C. Applicability Constraints

We recalled the Banach theorem for one mapping. Nevertheless, with our classifier not all equations in Table I first are contracting, second are relevant, third have attractors. Therefore, before applying the proposed DPA algorithm to our rate constrained system, we need to check that in each cell $\mathscr{C}_i$ at least one of the nine mappings in Table I is first a contraction whose attractor is within its applicability region, second the single mapping $(u_i^{O_i^{n+1}} \circ u_j^{O_j^n})$ which is relevant to the momentary interference scenario $(O_i^{n+1}; O_j^n)$.

*C.1) Existence of $\underline{\Gamma}^* = (\gamma_1^*, \gamma_2^*)$:* The mappings $u_i^k$ and $u_j^l$ in (12) are restricted to a region of applicability. Since $\Phi_i$ is composed by $u_i^k$ and $u_j^l$, $\Phi_i$ has also a region of applicability. Therefore, $\Phi_i$ can converge to its attractor $\gamma_i^*$ only if $\gamma_i^*$ exists and is within the applicability region of $\Phi_i$. An attractor, which is within the applicability region of its mapping, will be said *relevant*. The convergence of our algorithm needs that both $\Phi_1$ and $\Phi_2$ have *relevant* attractors. We show below that there always is at least one vector $(\gamma_1^*; \gamma_2^*)$ of *relevant* attractors.

Figure 2 illustrates the achievable SNR region $\mathscr{R}_i^*$. Actually, solid blue lines $(\mathscr{D}_i^k)_k$ illustrate the mappings $(u_i^k)_k$ within their applicability region, delimited by dash-dot red lines. On

Figure 3a both $\mathscr{R}_1^*$ and $\mathscr{R}_2^*$ are superposed. $\mathscr{D}_1^k$ and $\mathscr{D}_2^l$ are drawn respectively by dashed purple and solid blue lines, while applicability regions of $u_1^k$ and $u_2^l$ are delimited respectively by dotted green and dash-dot red lines. The nine pairs of regimes are captioned between brackets; their applicability region is differently coloured. A yellow star marks the crossed point $\underline{\Gamma}^* = (\mathscr{D}_1^k)_k \cap (\mathscr{D}_2^l)_l$. In effect, $\underline{\Gamma}^*$ coincides with the vector $(\gamma_1^*;\gamma_2^*)$ of attractors. Indeed, $\underline{\Gamma}^*$ is the single point of the region that simultaneously verifies $u_1^{O_1}$ and $u_2^{O_2}$ (geometric reason), so the vector $(\gamma_1^*;\gamma_2^*)$ also does (analytical reason). Besides, $\mathscr{D}_1^k$ and $\mathscr{D}_2^l$ are restricted, by construction, to their region of applicability; $\underline{\Gamma}^* = (\gamma_1^*;\gamma_2^*)$ is so certainly a vector of *relevant* attractors. The region $(O_1;O_2)$ within which $\underline{\Gamma}^*$ is located is named by $\underline{O}^*$. A geometrical reasoning could prove that $(\mathscr{D}_1^k)_k$ always crosses $(\mathscr{D}_2^l)_l$, whatever $\mathscr{P}_S$.

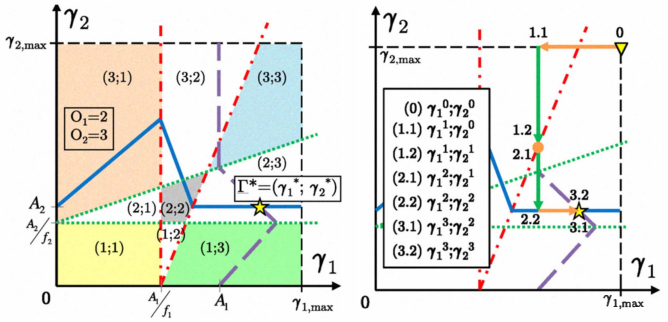


(a) Superposition of $\mathscr{R}_1^*$ and $\mathscr{R}_2^*$ (b) DPA "ping-pong" process

Fig. 3: $\mathscr{P}_S = \{1;1;2.5;1.5\}$: Vector $\underline{\Gamma}^*$ of *relevant* attractors

On Figure 3b, $\mathscr{C}_1$ starts the "ping-pong" process. Initial $\underline{\Gamma}^0$ is marked by a yellow downward-pointing triangle, while final $\underline{\Gamma}^*$ met after three iterations is marked by a yellow star. Orange horizontal and green vertical arrows respectively illustrate the update of $(\gamma_1^n)_n$ and $(\gamma_2^n)_n$. Steps are marked at arrows end: first the iteration counter, second the active cell. At step **1.2**, the second regime is relevant in $\mathscr{C}_2$ ($O_2^1 = 2$); the update of $\gamma_2^0$ with $u_2^2$ would like to join the diagonal blue line $\mathscr{D}_2^2$, but $\gamma_2^1$ must remain consistent with $\delta_1^1$ assumptions; so the diagonal red bound cannot be crossed. At step **2.1**, $\gamma_1^1$ is already optimal, so $\gamma_1^2 = \gamma_1^1$. At step **2.2**, $O_2^2 = 3$; the update $\gamma_2^2$ of $\gamma_2^1$ with $u_2^3$ joins lastly the horizontal blue line $\mathscr{D}_2^3$.

*C.2) Relevance of $\underline{O}^*$ and $(\Phi_1;\Phi_2)$:* We should consider $\Phi_i^{O^n}$ instead of $\Phi_i$. Indeed, Table I shows $\Phi_i$ intrinsically depends on interference regimes $(O_i^{n+1};O_j^n)$, while the updating process may lead to change $O_i^{n+1}$ and $O_j^n$ from one iteration to another. However, it exists a number $N$ of iterations such that $\forall n > N$, $O_i^n$ and $O_j^n$ do not change any more. $\Phi_1$ and $\Phi_2$ are in fact defined for this last pair of interference regimes, named by $\underline{O}^*$. $\Phi_i^{O^n}$ is just a transitional mapping before converge to $\Phi_i$. We prove first that $\underline{O}^*$ exists and is met, and second that $\Phi_1$ and $\Phi_2$ admit *relevant* attractors $\gamma_1^*$ and $\gamma_2^*$.

*Proof:* The Banach theorem states that $(u^n(x_0))_n$ converges to and only to $x^*$, whatever $x_0$, if $u$ is a contraction. Thus, as soon as the "ping-pong" process meets a pair $\underline{O}^n$ of regimes where $\Phi_1^{O^n}$ and $\Phi_2^{O^n}$ are contractions with *relevant* attractors, then the convergence will be ensured and $\underline{O}^n$ will not change any more. The existence of such a region with a vector $\underline{\Gamma}^*$ of *relevant* attractors was established in V-C.1. nevertheless, if the region $\underline{O}^*$ exists, $\underline{O}^*$ has to be met.

$(\gamma_1^n;\gamma_2^n)_n$ cannot remain in a region whose attractors are not *relevant*; such a region is indeed 'repellent'. Therefore, $(O_1^n;O_2^n)_n$ will change until $\underline{O}^*$ is met. Nevertheless, we could imagine that $(\gamma_1^n;\gamma_2^n)_n$ may oscillate between two repellent regions without ever meet $\underline{O}^*$. However, the transverse and successive updates of $(\gamma_1^n)_n$ and $(\gamma_2^n)_n$, combined with easy rules at regimes boundaries, prevent from such oscillations. As a consequence, $\underline{O}^*$ is always met. ■

*C.3) Is $\Phi_i$ a Contraction? :* Nevertheless, all previous results are useless if $\Phi_1$ or $\Phi_2$ is not contracting. Referring to Table I, $\Phi_i$ is either constant or a linear function. When $\Phi_i$ is constant, $\Phi_i$ is of course contracting. In case of linear functions, (11) is easily proved to be satisfied, as the slope $\tau_i$ of $\Phi_i$ is its Lipschitz constant; so $\Phi_i$ is a contraction $\Leftrightarrow (\tau_i < 1)$.

*a) $\underline{O}^* = (1;1)$:* The positivity of the attractor $\gamma_i^*$ proves that $\Phi_1$ and $\Phi_2$ are always contractions in $\underline{O}^* = (1;1)$.

$$\gamma_i^* = \frac{A_i(1 + A_j f_j)}{1 - \tau_i} > 0 \quad \Rightarrow \quad (1 - \tau_i) > 0$$

*b) $\underline{O}^* = (1;2)$ or $(2;1)$:* Slopes are $\tau_i = A_1 f_1 f_2$ and $\tau_j = A_2 f_1 f_2$. But $(\tau_i < 1)$ and $(\tau_j < 1)$ are not always satisfied. Thus, $(\gamma_i^n)_n$ may not converge in these regimes.

*c) $\underline{O}^* = (2;2)$:* The positivity of $\gamma_i^*$ can be used to compare $\tau_i = f_1 f_2$ to 1. This translates into (14).

$$\begin{cases} (1 - f_i f_j) > 0 \\ 1 - f_i > 0 \\ 1 - f_j > 0 \end{cases} \quad \text{or} \quad \begin{cases} (1 - f_i f_j) < 0 \\ 1 - f_i < 0 \\ 1 - f_j < 0 \end{cases} \tag{14}$$

In the first case, $\Phi_i$ is a contraction (since $\tau_i < 1$). The second case is a special scenario where regimes pairs $(2;2)$, $(2;3)$ and $(3;2)$ are simultaneously relevant (see Fig. 4): if $(\gamma_i^n)_n$ cannot converge in $(2;2)$ (as $\tau_i > 1$), the convergence is on the other hand ensured in $(2;3)$ or $(3;2)$ (see below).

*d) Other pairs $\underline{O}^*$:* In case of regimes $(1;3)$, $(3;1)$, $(2;3)$, $(3;2)$ and $(3;3)$, $\Phi_i$ is constant and so contracting.

*e) Conclusion:* To complete the proof, we recall that $\mathbb{R}^2$ is a non-empty complete metric space fitted with the euclidean metric. $(\gamma_i^n)_n$ is an iterated function sequence derived from $\Phi_i : \mathbb{R}^2 \to \mathbb{R}^2$. When both $\Phi_1$ and $\Phi_2$ are contracting, then the Banach theorem states the convergence in finite time of $(\gamma_1^n;\gamma_2^n)_n$, and so of our algorithm.

*C.4) Power Limitation:* Our system is power constrained by $(\mathbf{P_{1,max}};\mathbf{P_{2,max}})$. If at any iteration a power $P_i^n$ exceeds its limitation, then the process should be stopped. The convergence of the process may be not ensured; user transmission rejection or Time Sharing between cells can be applied.

### D. Initial Power Vector and Rate of Convergence

*D.1) Initial $\underline{P}^0$:* The Banach theorem says the initial value does not affect the final convergence. $\underline{P}^0 = (\mathbf{P_{1,max}};\mathbf{P_{2,max}})$ is so adopted. Nevertheless, the right case of (14) describes a scenario where regions $(2;2)$, $(2;3)$ and $(3;2)$ have all a

*relevant* vector $\underline{\Gamma}^*$. $\underline{P}^0$ may then lead to converge to one or another attractor, as attested on Figure 4 where we plot in green and magenta the convergence for two different $\underline{P}^0$.

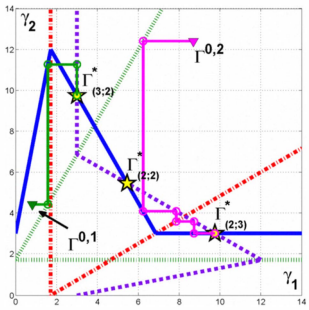


Fig. 4: $\mathscr{P}_S = \{2; 2; 1.75; 1.75\}$: 3 attractors $\underline{\Gamma}^*$.

*D.2) Rate of Convergence:* When the convergence is ensured ($\kappa < 1$), the convergence rate of $(\gamma_i^n)_n$ depends on the Lipschitz constant $\kappa$: the smaller $\kappa$ is, the faster $(\gamma_i^n)_n$ converges. This result is attested by Figure 5a which plots the number of iterations before convergence versus $\kappa$. The considered scenario is $\mathscr{P}_S = \{2; 2; f_1; 0.25\}$, while the initial vector is $\underline{\Gamma}^0 = (40; 20)$. Coefficient $f_1$ varies between 0 and 0.25: in these conditions, $\underline{\Gamma}^*_{(1;1)}$ is the only *relevant* attractor; $\kappa = A_1A_2f_1f_2$ in $\underline{O}^* = (1; 1)$ (see Tab.I). By varying $f_1$ while $A_1$, $A_2$ and $f_2$ are kept constant, we notice that the convergence is faster when $f_1$ (and so $\kappa$) is smaller. The convergence is besides met with at most 19 iterations and at least two iterations. Increasing $f_1$ beyond 0.25 causes $\underline{\Gamma}^*_{(1;1)}$ to be not relevant any more.

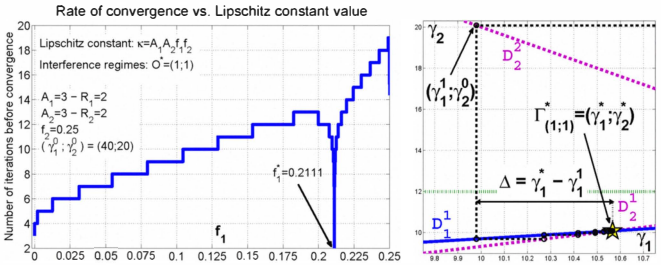


(a) Impact of Lipschitz constant value (b) Zoom in on $\underline{\Gamma}^*_{(1;1)}$

Fig. 5: Rate of convergence for attractor $\underline{\Gamma}^*_{(1;1)}$

However, a singular value $f_1^* = 0.2111$ seems to be optimal and in contradiction with the curve trend. Figure 5b shows regions $\mathscr{R}_1^*$ and $\mathscr{R}_2^*$ for this value $f_1^*$ and zooms in around $\underline{\Gamma}^*_{(1;1)}$. Equations of $\mathscr{D}_2^1$ and $\mathscr{D}_2^2$ vary with $f_1$ (see 12), so the gap $\Delta = |\gamma_1^* - \gamma_1^1|$ does. The value $f_1^*$ lets $\gamma_1^1$ equal the attractor $\gamma_1^*$ in one iteration ($\Delta = 0$), whereas for all other values of $f_1$ the convergence to $\gamma_1^*$ needs several iterations.

Requested conditions for convergence were established in V-C.3. For some scenarios $\mathscr{P}_S$ where $\underline{\Gamma}^*$ is located within $(1; 2)$ or $(2; 1)$, convergence may not be ensured naturally. However, source $s_i$ can quickly detect the non-convergence and reacts. Indeed, it exists in this case a number $n_1$ of iterations such that for every $n > n_1$, $(P_i^n)_n$ oscillates between a couple of powers. $s_i$ has then simply to notify $s_j$ and Time Sharing or transmission rejection is applied.

## VI. Conclusion

In this paper, we investigate distributed power allocation (DPA) techniques best suited for interference limited and QoS constrained cellular networks. First, we propose a simplified and effective interference classification method which can be performed by each destination without relying on a central decision maker. Then, we design a novel DPA mechanism which exploits the proposed classification of interference to minimize the power budget in each cell. Our analytical and numerical evaluations show that the proposed DPA algorithm most of the time converges while QoS constraints are met. Future works will focus on a generalization to more than two cells, as well as on a finer investigation of rate convergence.

## Acknowledgments

This work has been performed in the framework of the ICT project ICT-4-248523 BeFEMTO, which is partly funded by the European Union.

## References

[1] Y. Xiang, J. Luo and C. Hartmann, "Inter-cell interference mitigation through flexible resource reuse in OFDMA based communication networks," *Proc. EW 2007*, pp. 1–7, Apr. 2007.

[2] D. Tse and P. Viswanath, "Fundamentals of wireless communication," Cambridge University Press, May 2005.

[3] J. Boutros, N. Gresset, L. Brunel and M. Fossorier, "Soft-input soft-output lattice sphere decoder for linear channels," *IEEE GLOBECOM 2003*, pp. 1583–1587, Dec. 2003.

[4] K. Gomadam, V.R. Cadambe and S.A. Jafar, "Approaching the capacity of wireless networks through distributed interference alignment," *IEEE GLOBECOM 2008*, pp. 1–6, Nov. 2008.

[5] S.M. Perlaza, M. Debbah, S. Lasaulce and J.-M. Chaufray, "Opportunistic interference alignment in MIMO interference channels," *IEEE PIMRC 2008*, pp. 1–5, Sep. 2008.

[6] A.J. Goldsmith and S.-G. Chua, "Adaptive coded modulation for fading channels," *IEEE Trans. Comm.*, vol. 46, no. 5, pp. 595–602, May 1998.

[7] T. Cover and J. Thomas, "Elements of Information Theory," *Wiley*, 2006.

[8] S. Boyd and L. Vandenberghe, "Convex optimization," *Cambridge University Press*, 2006.

[9] M. Chiang, C.W. Tan, D.P. Palomar, D. O'Neill and D. Julian, "Power control by geometric programming," *IEEE Trans. Wireless Comm.*, vol. WC-6, no. 7, pp. 2640-2651, Jul. 2007.

[10] S. Kandukuri and S. Boyd, "Optimal power control in interference-limited fading wireless channels with outage-probability specifications," *IEEE Trans. Wireless Comm.*, vol. WC-1, no. 1, pp.46–55, Jan. 2002.

[11] C.-H. Yih and E. Geranotis, "Centralized power allocation algorithms for OFDM cellular networks," *IEEE MILCOM 2003*, pp. 1250–1255, Oct. 2003.

[12] A. Gjendemsjo, D. Gesbert, G.E. Oein and S.G. Kiani, "Optimal power allocation and scheduling for two-cell capacity maximization," *WiOPT 2006*, vol. 95, no. 12, pp. 1–6, Apr. 2006.

[13] R.H. Etkin, D.N.C. Tse and H. Wang, "Gaussian interference channel capacity to within one bit," *IEEE Trans. Info. Theory*, vol. IT-54, no. 12, pp. 5534–5562, Dec. 2008.

[14] S.A. Jafar and S. Vishwanath, "Generalized degrees of freedom of the symmetric Gaussian K user interference channel," *submitted to arXiv*, Apr. 2008, available at http://arxiv.org/abs/0804.4489.

[15] T.S. Han and K. Kobayashi, "A new achievable rate region for the interference channel," *IEEE Trans. Info. Theory*, vol. IT-27, no. 1, pp. 49–60, Jan. 1981.

[16] T.M. Cover, A. El Gamal and M. Salehi, "Multiple access channel with arbitrarily correlated sources," *IEEE Trans. Info. Theory*, vol. IT-26, no. 6, pp. 648–657, Nov. 1980.

[17] A.S. Motahari and A.K. Khandani, "Capacity bounds for the Gaussian interference channel," *IEEE Trans. Info. Theory*, vol. IT-55, no. 2, pp. 620–643, Feb. 2009.

[18] A.B. Carleial, "A case where interference does not reduce capacity (Corresp.)," *IEEE Trans. Info. Theory*, vol. IT-21, no. 5, pp. 569–570, Sep. 1975.

[19] A. Granas and J. Dugundji, "Fixed point theory," *Springer Verlag*, 2003.